Title
Characterization of Fourier domain modelocked wavelength swept laser for optical coherence tomography imaging

Journal
Optics Express, 16(6)

ISSN
1094-4087

Authors
Jeon, Min Yong
Zhang, Jun
Chen, Zhongping

Publication Date
2008-03-06

DOI
10.1364/OE.16.003727

Peer reviewed

Characterization of Fourier domain mode-locked wavelength swept laser for optical coherence tomography imaging

Min Yong Jeon[1,2], Jun Zhang[1], and Zhongping Chen[1,3]

[1.] *Beckman Laser Institute, University of California, Irvine, Irvine, California 92612*
[2.] *Department of Physics, Chung Nam National University, Daejeon, Korea 305-764*
[3.] *Department of Biomedical Engineering, University of California, Irvine, Irvine, California 92612*
Corresponding authors: z2chen@uci.edu, myjeon@cnu.ac.kr

Abstract: We present characteristics of a wavelength swept laser with a scanning fiber Fabry-Perot filter at 1300 nm. We investigate the dependence of the scanning frequencies in the swept laser. In conventional wavelength swept lasers, the relative intensity of the laser output decreases significantly as the scanning frequency increases. The peak wavelength of the output spectrum is red-shifted due to the nonlinear frequency downshifting in the semiconductor optical amplifier (SOA). In the Fourier domain mode-locked (FDML) wavelength swept laser, we investigate transient intensity profiles and the full width at half maximum in response to the injection currents and detuning of the scanning frequency. The degradation of the scanning range of the swept laser is caused by the deviation from the scanning frequency at 45.6 kHz. In addition, transient intensity profiles show significant asymmetric behavior in response to the detuned frequencies. Finally, the axial resolution and sensitivity as a function of imaging depth are analyzed for both forward and backward scans. With the FDML laser, the detection sensitivity up to 102 dB is achieved for the backward scans. The backward scans exhibit higher axial resolution and sensitivity than the forward scan.

OCIS codes: (110.4500) Optical coherence tomography; (120.3180) Interferometry; (140.3510) lasers, fiber; (140.3600) Lasers, tunable

References and links

1. D. Huang, E. A. Swanson, C. P. Lin, J. S. Schuman, W. G. Stinson, W. Chang, M. R. Hee, T. Flotte, K. Gregory, C. A. Puliafito, and J. G. Fujimoto, "Optical Coherence Tomography," Science **254**, 1178-1181, (1991).
2. M. A. Choma, M. V. Sarunie, C. Yang, and J. Izatt, "Sensitivity advantage of swept source and Fourier domain optical coherence tomography," Opt. Express **11**, 2183-2189, (2003).
3. G. Hausler and M. W. Lindner, "Coherence radar and spectral radar- new tools for dermatological diagnosis," J. Biomed. Opt. **3**, 21-31 (1998).
4. R. Leitgeb, C. Hitzenberger, and A. Fercher, "Performance of fourier domain vs. time domain optical coherence tomography," Opt. Express **11,** 889-894 (2003).
5. S. H. Yun, G. Tearney, J. de Boer, N. Iftimia, and B. Bouma, "High-speed optical frequency-domain imaging," Opt. Express **11**, 2953-2963 (2003).
6. J. Zhang, J. S. Nelson, and Z. P. Chen, "Removal of a mirror image and enhancement of the signal-to-noise ratio in Fourier-domain optical coherence tomography using an electro-optic phase modulator," Opt. Lett. **30**, 147-149 (2005).
7. R. Huber, M. Wojtkowski, and J. G. Fujimoto, "Fourier domain mode locking (FDML): A new laser operating regime and applications for optical coherence tomography," Opt. Express **14**, 3225-3237 (2006).
8. M. A. Choma, K. Hsu, and J. A. Izatt, "Swept source optical coherence tomography using an all-fiber 1300-nm ring laser source," J. Biomed. Opt. **10**, 044009 (2005).
9. W. Y. Oh, S. H. Yun, G. J. Tearney, and B. E. Bouma, "Wide tuning range wavelength-swept laser with two semiconductor optical amplifiers," IEEE Photon. Technol. Lett. **17**, 678-680 (2005).
10. S. H. Yun, C. Boudoux, G. J. Tearney, and B. E. Bouma, "High-speed wavelength-swept semiconductor laser with a polygon-scanner-based wavelength swept filter," Opt. Lett. **28**, 1981-1983 (2003).

#91728 - $15.00 USD Received 14 Jan 2008; revised 16 Feb 2008; accepted 16 Feb 2008; published 6 Mar 2008

11. R. Huber, M. Wojtkowski, K. Taira, J. G. Fujimoto, and K. Hsu, "Amplified, frequency swept lasers for frequency domain reflectometry and OCT imaging: design and scaling principles," Opt. Express **13**, 3513-3518 (2005).
12. S.-W Lee, C. S. Kim, and B.-M. Kim, "External line-cavity wavelength-swept source at 850 nm for optical coherence tomography," IEEE Photon. Technol. Lett. **19**, 176-178 (2007).
13. A. Bilenca, S. H. Yun, G. J. Tearney, and B. E. Bouma, "Numerical study of wavelength-swept semiconductor ring lasers: the role of refractive-index nonlinearities in semiconductor optical amplifiers and implications for biomedical imaging applications," Opt. Lett. **31**, 760-762 (2006).
14. D. C. Adler, R. Huber, and J. G. Fujimoto, "Phase-sensitive optical coherence tomography at up to 370,000 lines per second using buffered Fourier domain mode-locked lasers," Opt. Lett. **32**, 626-628 (2007).
15. A. G. Podoleanu, "Unbalanced versus balanced operation in an optical coherence tomography system," Appl. Opt. **39**, 173-182 (2000).
16. J. Zhang, Q. Wang, B. Rao, and Z. Chen, "Swept laser source at 1 μm for Fourier domain optical coherence tomography," Appl. Phys. Lett. **89**, 073901 (2006).
17. J. Zhang and Z. Chen, "In vivo blood flow imaging by a swept laser source based Fourier domain optical Doppler tomography," Opt. Express **13**, 7449-7457 (2005).
18. R. Huber, D. C. Adler, and J. G. Fujimoto, "Buffered Fourier domain mode locking: unidirectional swept laser sources for optical coherence tomography imaging at 370,000 lines/s," Opt. Lett. **31**, 2975-2977 (2006).
19. D. C. Adler, Y. Chen, R. Huber, J. Schmitt, J. Connolly, and J. C. Fujimoto, "Three-dimensional endomicroscophy using optical coherence tomography," Nature Photonics **1**, 709-716 (2007).

1. Introduction

Optical coherence tomography (OCT) is a noninvasive, noncontact imaging modality that uses coherent gating to obtain near histologic level resolution, cross-sectional images of tissue microstructure in three dimensions [1]. Recent developments of Fourier domain OCT (FDOCT), also known as swept source OCT, have improved the imaging speed and detection sensitivity of OCT systems [2-7]. A key technology in obtaining a tomographic image in FDOCT is an optical source [8-12]. It is desirable to obtain a broader spectrum and faster scanning rate to increase the axial resolution and the acquisition rate for 3-D imaging in the OCT system because the resolution is inversely proportional to the bandwidth of the laser source, and the scanning rate is determined by the A-line acquisition rate. The wide bandwidth wavelength swept laser has been developed for high-speed, high-resolution FDOCT using various methods, which includes an optical Fabry-Perot scanning filter, a grating with a polygon rotating mirror, and an external cavity scheme [10-12].

In general, the scanning speed of a conventional swept light source is limited by both the tuning speed of the optical filter and laser cavity lifetime. In the conventional wavelength swept laser with low scanning frequency (<1 kHz), there is no significant decrease in the output spectrum and the temporal intensity profile for both forward (shorter to longer wavelength) and backward (longer to shorter wavelength) scans. However, higher sweeping frequencies of more than 2 kHz have a significant peak power imbalance between the forward and the backward scan due to the nonlinearity of the SOA [11, 13]. R. Huber, *et al*., [7] recently employed the Fourier domain mode-locked (FDML) wavelength swept laser to increase the scanning rate without asymmetric behavior. With the FDML technology, the limitation of the maximum scanning rate due to the laser cavity lifetime can be overcome by driving the optical filter synchronously with the optical round-trip time of the light wave in the cavity. The FDML swept source has the advantages of high scanning speed, narrow linewidth, and high phase stability [14]. In this manuscript, we report detailed characteristics of a wavelength swept laser in the 1300 nm wavelength region. For the conventional wavelength swept laser, we investigate the dependence of the scanning frequency in the laser. We demonstrate effects of the detuning frequency and injection currents in the FDML swept laser. The scanning frequency of the FDML swept laser is 45.6 kHz, which is the same as the fundamental longitudinal frequency of the total laser cavity. The deviation from the scanning frequency causes the decrease of the full width of the swept laser. In addition, the transient intensity profiles show significant asymmetric characteristics in response to the detuned frequency. The transient intensity profiles of the forward and the backward scans are investigated in response to the applied injection currents at 45.6 kHz. We analyze the axial

#91728 - $15.00 USD Received 14 Jan 2008; revised 16 Feb 2008; accepted 16 Feb 2008; published 6 Mar 2008

resolution and sensitivity as a function of imaging depth for both forward and backward scans. The maximum sensitivity of the FDML swept laser is 102 dB at a depth of 0.25 mm and is decreased by 10 dB at a 2 mm imaging depth for the backward scans. The backward scans exhibit higher axial resolution and sensitivity than the forward scan.

2. Experimental set-up

The wavelength swept laser source is constructed on the basis of the conventional ring laser cavity. Figure 1 shows the experimental set-up for the wavelength swept laser and an OCT imaging system. The wavelength swept laser consists of a semiconductor optical amplifier (SOA; from InPhenix, Inc.), two isolators, a 30 % output fiber coupler, and a scanning fiber Fabry-Perot tunable filter (FFP-TF; from Micron Optics, Inc.). Two isolators are used to operate unidirectional propagation in the laser cavity. The output from the wavelength swept laser is monitored with an optical spectrum analyzer and a sampling oscilloscope via 30 % fiber coupler. In order to operate the FDML wavelength swept laser at a higher frequency, a 4.5 km long dispersion-managed SMF-28e fiber is added to the laser cavity. The total cavity length, including all fiber components, is ~ 4,506 m. At this cavity length, the applied scanning frequency is 45.6 kHz. The sweeping speed can be increased if a higher frequency PZT driver is used. The current system can be scaled to higher frequencies with the high frequency driver. The FFP-TF has a free spectral range of ~ 210 nm at 1300 nm and a linewidth of ~ 0.2 nm. The scanning FFP-TF is driven at the matching longitudinal frequency of the laser cavity. Thus, the traveling light from one frequency sweep propagates through the laser cavity. The corresponding mismatched dispersion is less than 2.1 ns for a wavelength range from 1240 nm to 1380 nm [7].

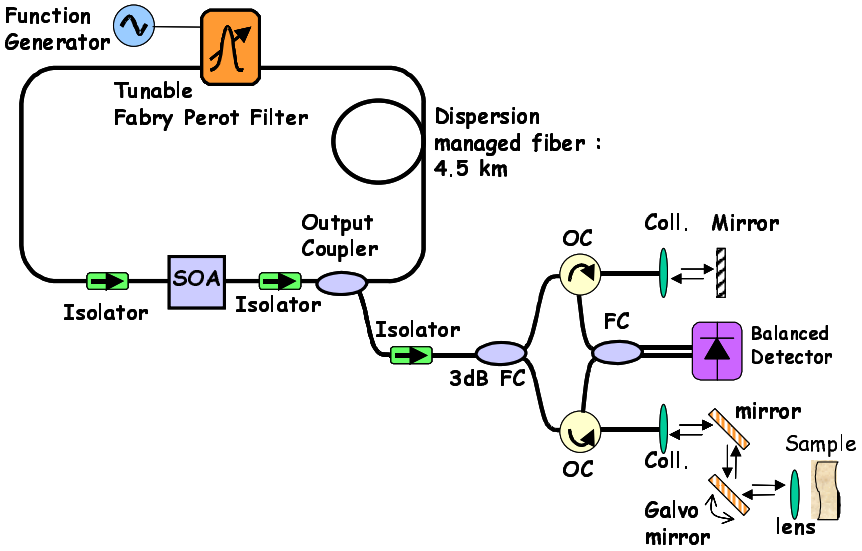

Fig. 1. Experimental set-up for wide-bandwidth, high-speed of a FDML wavelength swept laser and an OCT system. (PC: polarization controller; FC: fiber coupler; OC: optical circulator; SOA: semiconductor optical amplifier; Coll.: collimator).

The OCT imaging system is constructed based on a Mach-Zehnder interferometer using a 3 dB fiber coupler. The swept source OCT imaging system consists of two 3 dB fiber couplers, two optical circulators, two collimators, a mirror, a Galvanometer mounted mirror, and a balanced detector. The reflected beams from both reference and sample arms are coupled through two optical circulators. The balanced detector measures the signal via a fiber coupler. The balanced detection system using a 3 dB fiber coupler increases the signal-to-noise ratio of the OCT system [15, 16]. In the detection arm, the time fringe signal is collected

#91728 - $15.00 USD Received 14 Jan 2008; revised 16 Feb 2008; accepted 16 Feb 2008; published 6 Mar 2008

by the photodetectors with detection bandwidth of 75 MHz (PDB120C, Thorlabs) and is digitized by a 14 bit data acquisition board sampling at 100 M samples/s. The number of data points for each A-line data acquisition is 600. The signal that drives FFP-TF also generates an A-line trigger signal, which is used to initiate the data acquisition process for each A-line. The complex analytical depth encoded signal is converted from the collected time fringe signal by fast Fourier transform. The structure image is reconstructed from the amplitude term of the complex depth encoded signal.

3. Experimental results

3.1. Conventional wavelength swept laser at lower frequencies

In this experiment, we investigate the dependence of the sweeping frequency in the conventional wavelength swept laser with a scanning FFP-TF by removing the long dispersion-managed SMF-28e fiber in Fig. 1. Figure 2 shows the normalized relative intensity of the output power versus the scanning frequency in the conventional wavelength swept laser. The normalized relative intensity is measured by the spectral output and it is compared to the intensity of the lowest frequency in the wavelength domain. As the sweeping frequency increases, the relative intensity decreases significantly. The relative intensity around 5 kHz is decreased by 10 dB compared to 1 kHz. At 15 kHz sweeping frequency, it is dramatically decreased by 20 dB compared to 1 kHz as shown in Fig. 2. Therefore, the output power of the conventional swept laser at frequencies greater than 5 kHz would not be sufficient for OCT application. It may require a booster amplifier after output of the swept laser as reported by Huber, *et al.*, [11].

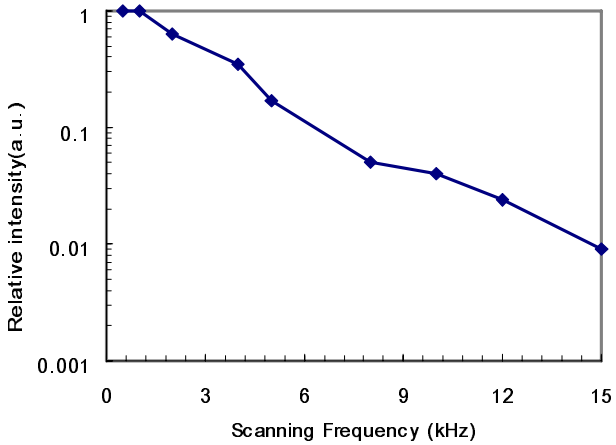

Fig. 2. Relative intensity of the output power in the spectral domain versus the scanning frequency for the conventional wavelength swept laser.

With a sweeping frequency of less than 1 kHz, there is no decrease in the spectral power and the temporal intensity profile for both forward and backward scans as shown in Figs. 3(a) and 3(b). However, higher scanning frequencies of more than 2 kHz show a significant peak power imbalance between the forward scan and the backward scan as shown in Figs. 3(d), 3(f), and 3(h). This asymmetry is due to nonlinearity of the gain medium [13]. Bilenca, *et al.*, reported the laser characteristics versus scanning speed with numerical analysis of the wavelength swept SOA ring laser [13]. As the sweeping frequency increases, the output spectra exhibit the asymmetric behavior [11]. Therefore, the peak power of the forward scan is higher than that of the backward scan. There is a considerable power decrease in the optical spectra as the scanning frequency increases as shown in Fig. 3. The peak power of the backward scan at 8 kHz is decreased as much as 50 % compared to the forward scan as shown in Fig. 3(f). In order to use both forward and backward scans, the peak powers should be similar in their temporal profiles. It should be noted that the comparable backward scan

#91728 - $15.00 USD Received 14 Jan 2008; revised 16 Feb 2008; accepted 16 Feb 2008; published 6 Mar 2008

intensity could be achieved using a booster SOA at much higher frequency sweeping rates [11]. Therefore, the conventional scanning FFP-TF wavelength swept laser without booster amplifier will be limited to a 1 kHz scanning rate when both forward and backward scan are used.

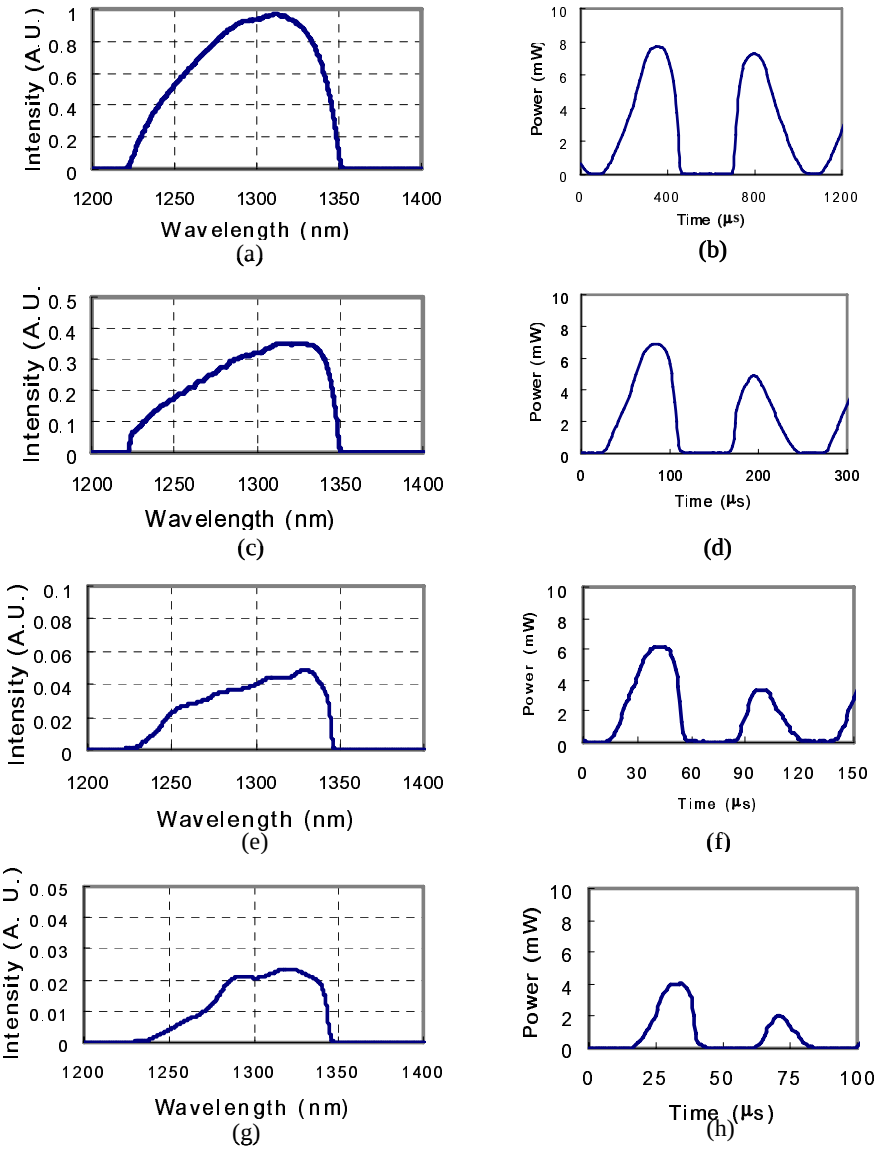

Fig. 3. Optical spectra and temporal intensity profiles of (a) and (b) at 1 kHz; (c) and (d) at 4 kHz; (e) and (f) at 8 kHz; (g) and (h) at 12 kHz, respectively.

3.2. Fourier mode-locked wavelength swept laser at a higher frequency

In these experiments, we investigate the characteristics of the FDML wavelength swept laser. Figure 4(a) shows the relationship between the scanning bandwidth and the different injection currents of the SOA at 45.6 kHz. The achieved maximum scanning bandwidth of the FDML laser is ~ 100 nm at 360 mA injection current of the SOA. At the operating current of 300 mA, a 3 dB scanning bandwidth of over 90 nm is achieved. Figure 4(b) shows the output spectra of

#91728 - $15.00 USD Received 14 Jan 2008; revised 16 Feb 2008; accepted 16 Feb 2008; published 6 Mar 2008

the wavelength swept laser in response to the applied injection currents. It shows the effect of the applied current on the gain bandwidth spectrum. The spectral shapes are almost the same when the injection currents are decreased even though the 3 dB scanning bandwidths are reduced. However, the center wavelengths are shifted slightly to the shorter wavelength. Figure 4(c) shows the transient intensity profiles of different applied injection currents of the SOA at a sweeping rate of 45.6 kHz. The peak power at the injection current of 360 mA is over 7.5 mW for both forward and backward scans. The average output power measured by optical power meter is ~ 4.8 mW. Similar to Fig. 3(b), the intensity profile shapes show almost no change. However, the amplitudes are gradually reduced as the injection currents are decreased.

The scanning bandwidth of the FDML wavelength swept laser depends on the driving frequency of the scanning FFP-TF. Figure 5 shows the variations in scanning bandwidth of the swept laser in response to detuned frequency of the scanning FFP-TF at the typical SOA operating injection current of 300mA. The detuned frequency is measured at the fundamental longitudinal frequency of the total laser cavity. Within the frequency detuning of ±2 Hz, the measured bandwidth is over 90 nm. However, the 3 dB scanning bandwidth at a frequency more than ±10 Hz detuning is decreased below the 80 nm scanning bandwidth. Therefore, for optical performance of FDML laser, the scanning frequency should be within ±2 Hz from the fundamental longitudinal frequency of the total laser cavity.

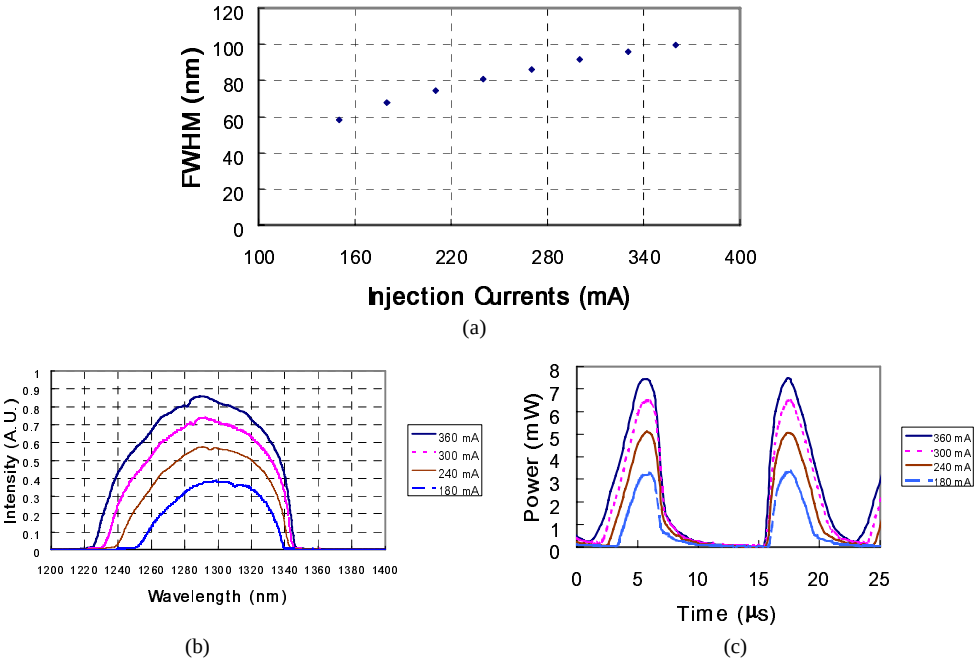

Fig. 4. (a). Scanning bandwidth at half maximum of the swept laser output versus injection current of the SOA in the laser cavity, (b) optical spectra of the swept laser according to different injection currents, and (c) temporal intensity profiles of the swept laser according to different injection currents in the time domain.

#91728 - $15.00 USD Received 14 Jan 2008; revised 16 Feb 2008; accepted 16 Feb 2008; published 6 Mar 2008

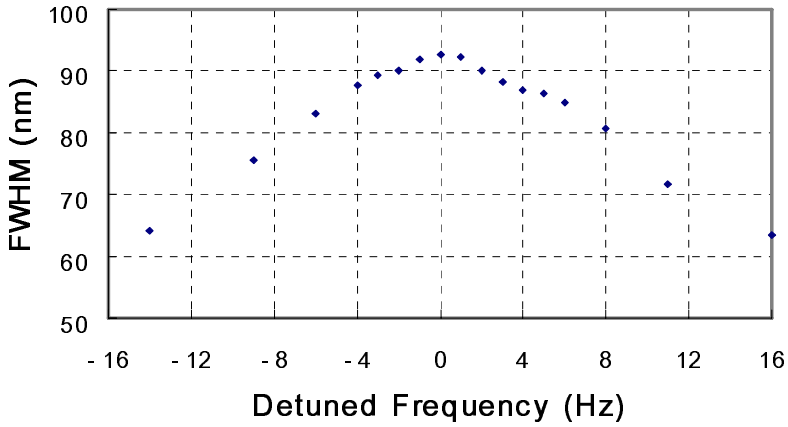

Fig. 5. Scanning bandwidth vs. frequency detuning from 45.6 kHz which is the same as the fundamental longitudinal frequency of the total laser cavity.

We also investigated the effects of the optical spectra and temporal intensity profiles of the wavelength swept laser with detuned scanning frequency. The peak power during the forward and backward scans is measured as a function of the detuned frequency in the FDML wavelength swept laser as shown in Fig. 6. The results show an asymmetric behavior for forward and backward scan when filter swept frequency is detuned from the longitudinal cavity frequency. For the positive detuned frequency from 45.6 kHz, the peak powers of the backward scan decreases much faster than that of the forward scan. However, for negative detuned frequency, the peak powers of the forward scan decreases much faster than that of the backward scan. This asymmetric behavior can be explained by the nonlinearity in the gain medium that tends to produce a frequency downshift (wavelength upshift) in energy [13].

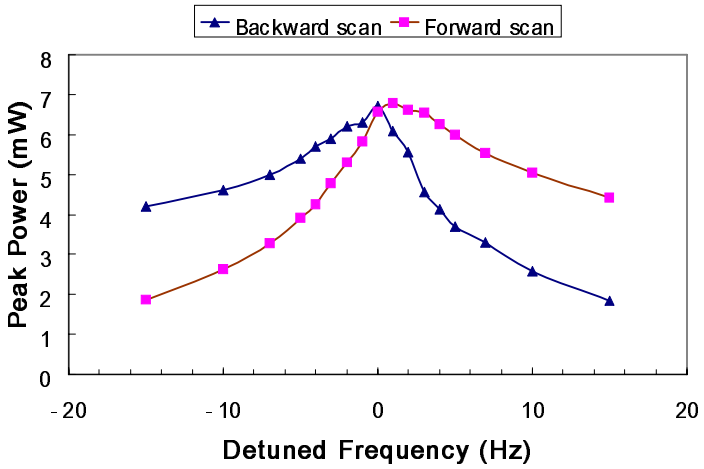

Fig. 6. Peak output power measured as a function of the detuned frequency from 45.6 kHz.

#91728 - $15.00 USD Received 14 Jan 2008; revised 16 Feb 2008; accepted 16 Feb 2008; published 6 Mar 2008

Figure 7 shows the schematic diagram of the wavelength scanning process in response to the detuned frequency. Let's assume that λ_0 is the center wavelength of the filter when photons start to propagate through the gain medium and cavity. For the positive detuning, the time of one frequency swept of filter is shorter than the roundtrip traveling time of photons in the cavity Thus, when photons return at the filter after one circular trip, the center wavelength of the filter is at $\lambda_0 + \Delta\lambda$ for forward scan and $\lambda_0 - \Delta\lambda$ for backward scan as shown in Fig. 7(a). Since photons are wavelength upshifted when passing the gain medium due to nonlinearity, more photons in forward scan can pass through the filter than backward scan. As a result, the peak power of forward scan is higher than backward scan. On the other hands, for negative detuning, the time of one frequency swept of filter is longer than the roundtrip traveling time of photons in the cavity. Thus, when photons return at the filter after one circular trip, the center wavelength of the filter is at $\lambda_0 - \Delta\lambda$ for forward scan and $\lambda_0 + \Delta\lambda$ for backward scan as shown in Fig. 7(b). Since photon wavelengths are upshifted when passing the gain medium due to nonlinearity, more photons for backward scans can pass through the filter than in forward scans. The peak power of the backward scan is much higher than the forward scan for negative detuning. The results also indicate that the maximum peak power is reached at ± 0.5 Hz detuning for forward and backward scans, respectively. This can also be explained by nonlinearity in the gain medium [13].

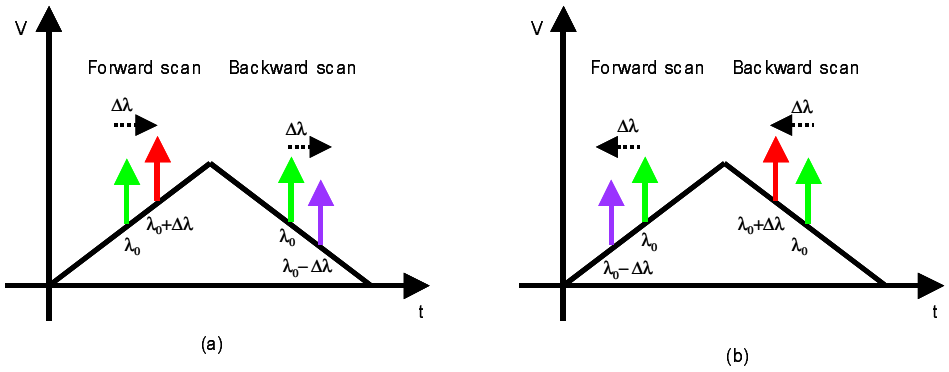

Fig. 7. Schematic diagram of the wavelength scanning process in response to the detuned frequency (a) Positive detuning; (b) negative detuning.

Figures 8(a) and 8(b) show the optical spectra and transient intensity profiles, respectively, according to the decrease of the detuning frequencies from 45.6 kHz. In this experiment, the applied current of the SOA is 300 mA. The optical spectra vary significantly as the detuning frequencies decrease from 45.6 kHz. The transient intensity profiles for the 45.6 kHz have the same peak powers for both forward and backward scans. However, as the detuned frequency decreases from 45.6 kHz, there is an asymmetric behavior for the temporal intensity profile between forward and backward scans as shown in Fig. 8(b). The peak power of the forward profile is decreased more than that of the backward profile. For the detuned frequency of 10 Hz, the peak power of the forward scan is reduced by 50 % compared to the backward scan. Figures 8(c) and 8(d) show the optical spectra and transient intensity profiles according to the increasing of the detuning frequencies from 45.6 kHz, respectively. It has the same characteristics of Figs. 8(a) and 8(b). In this case, for the detuned frequency of 10 Hz, the peak power of the backward scan is reduced by 50 % compared to the forward scan.

#91728 - $15.00 USD Received 14 Jan 2008; revised 16 Feb 2008; accepted 16 Feb 2008; published 6 Mar 2008

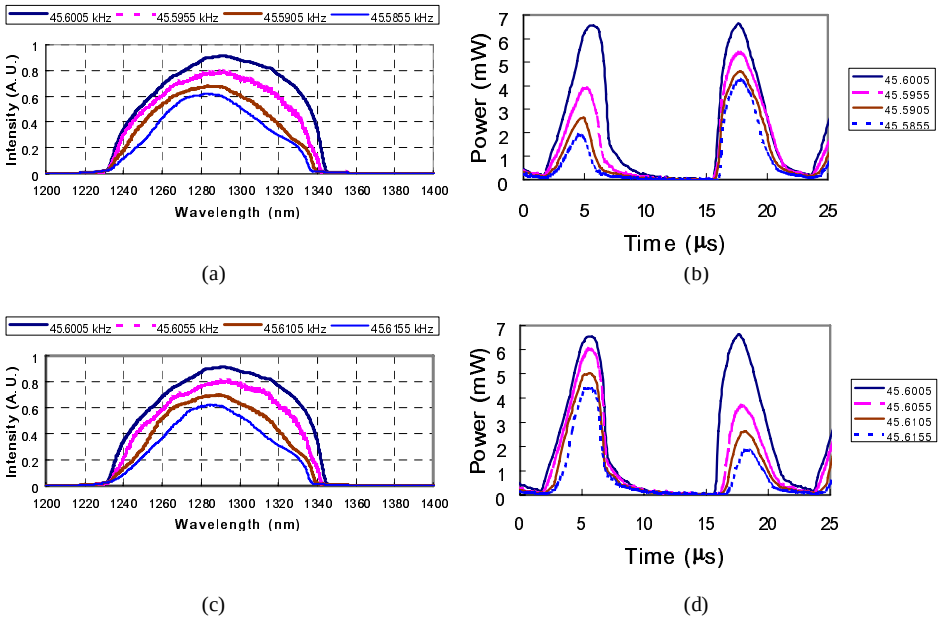

Fig. 8. (a). Optical spectra and (b) temporal intensity profiles according to the negative frequency detuning from 45.6 kHz; (c) optical spectra and (d) temporal intensity profiles according to the positive frequency detuning from 45.6 kHz.

In order to get an OCT image, dispersion and non-linear wave-number(k) should be compensated since dispersion mismatch in sample and reference arms would broaden the coherence function. It will cause degradation of the axial resolution of the system. In our swept source OCT system, the nonlinear phase function in wave number space is calibrated with a sample reflector to compensate for dispersion. 5% of the laser output was split and propagated through a 100 GHz fiber Fabry-Perot (FFP) interferometer (Micron Optics) to generate comb signals for dynamic calibration of the swept wavenumber function that is essential for rigorous conversion from time to wavenumber space [17]. Figure 9(a) shows the point spread function measured by a partial reflector using a Mach-Zehnder interferometer. It was measured under the FDML swept laser with 300 mA applied current and the scanning rate of 45.6 kHz. The measured axial resolution of the FDML wavelength swept laser at 45.6 kHz is 9.8 μm in air for the backward scan. It corresponds to the effective axial resolution of 7.0 μm in tissue (n=1.4). The analysis of the axial resolution and imaging depth are very important to understand imaging performance of the system. Figure 9(b) shows the axial resolution as a function of depth for the forward and backward scans. It should be noted that the backward scans exhibit a superior axial resolution with increasing depth when compared with the forward scans. This is because the backward scans have reduced noise when compared with forward scans, despite both scans having equal transient power characteristics [18]. The axial resolution of the backward scans has around 10 μm at 1.5 mm imaging depths.

#91728 - $15.00 USD Received 14 Jan 2008; revised 16 Feb 2008; accepted 16 Feb 2008; published 6 Mar 2008

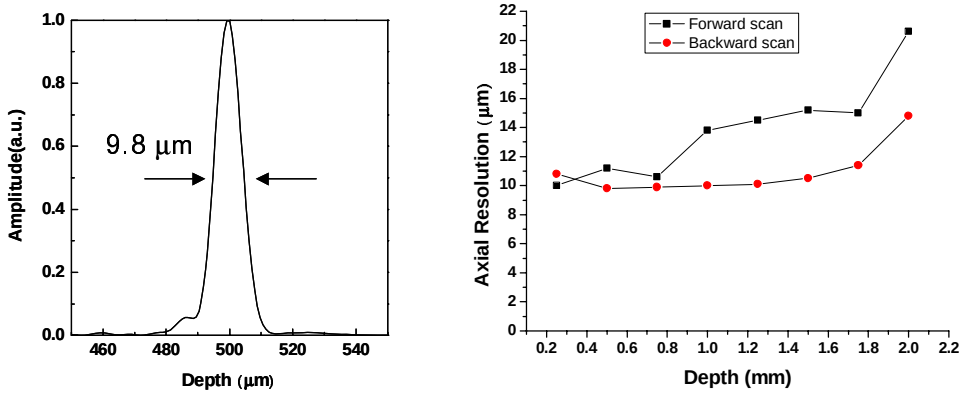

(a) (b)

Fig. 9. (a). Forward scan point spread function, (b) axial resolution as a function of depth.

In order to characterize the performance of the FDML laser, we also measured sensitivity of the OCT system based on the FDML swept laser. Figure 10 shows the measured OCT point spread functions for the forward and backward scans. Sensitivity is measured by placing a partial reflector with a measured attenuation of 56.7 dB in the sample arm. The maximum sensitivity of the forward scan is 98.7 dB at a depth of 0.25 mm as shown in Fig. 10(a). A decrease of about 12.8 dB within a depth range of 2mm is measured. For the backward scan, the maximum sensitivity is 102 dB at a depth of 0.25 mm. The sensitivity at a depth of 2 mm is 92 dB which is reduced by 10 dB from the maximum sensitivity as shown in Fig. 10(b). Similar to the axial resolution, the backward scans exhibit a superior sensitivity with increasing depth when compared with the forward scans [18]. R. Huber, *et al.*, recently proposed and demonstrated the technology of the buffered FDML wavelength swept laser in order to improve the sensitivity and dynamic range in the OCT system [18, 19].

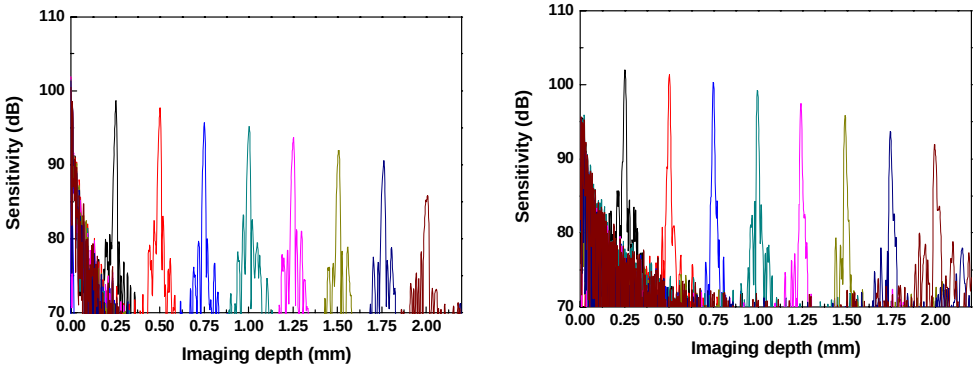

(a) (b)

Fig. 10. OCT point spread functions of a partial reflector placed in the sample arm at different imaging depths: (a) forward scans; (b) backward scans.

#91728 - $15.00 USD Received 14 Jan 2008; revised 16 Feb 2008; accepted 16 Feb 2008; published 6 Mar 2008

4. Conclusion

The characteristics of the wavelength swept laser with a scanning Fabry-Perot tunable filter were demonstrated. In the conventional wavelength swept laser at high sweeping frequency, the relative intensity decreased significantly and the output spectra showed asymmetric behavior due to the nonlinear frequency downshifting mechanism in the SOA. We investigated characteristics of a Fourier domain mode-locked (FDML) wavelength swept laser. The transient intensity profiles were investigated according to the applied injection currents at 45.6 kHz. The deviation from the scanning frequency at 45.6 kHz caused degradation of the full width of the swept laser. In addition, transient intensity profiles showed significant asymmetric characteristics according to the detuned frequency from the 45.6 kHz. The axial resolution and sensitivity as a function of imaging depth were analyzed for both forward and backward scans. We achieved the detection sensitivity up to 102 dB for the backward scans with the FDML swept laser. The measured axial resolution and sensitivity of the backward scans exhibited superior results than those from the forward scans.

Acknowledgments

This work was supported by research grants from the National Institutes of Health (EB-00293, CA-91717, and RR-01192), Air Force Office of Scientific Research (FA9550-04-1-0101), the Beckman Laser Institute Endowment, and the Korea Science and Engineering Foundation (KOSEF) grant funded by the Korea government (MOST) (R01-2007-000-20556-0). M. Y. Jeon was supported by research grants from the International Studies & Programs, Chungnam National University, Korea.

#91728 - $15.00 USD Received 14 Jan 2008; revised 16 Feb 2008; accepted 16 Feb 2008; published 6 Mar 2008